Store-operated Ca^{2+} entry during intracellular Ca^{2+} release in mammalian skeletal muscle

Bradley S. Launikonis[1,2] and Eduardo Ríos[1]

[1] *Section of Cellular Signalling, Department of Molecular Biophysics and Physiology, Rush University Medical Center, 1750 W. Harrison Street, Chicago, IL 60612, USA*

[2] *School of Biomedical Sciences, University of Queensland, Brisbane, Queensland, 4072, Australia*

Store-operated Ca^{2+} entry (SOCE) is activated following the depletion of internal Ca^{2+} stores in virtually all eukaryotic cells. Shifted excitation and emission ratioing of fluorescence (SEER) was used to image mag-indo-1 trapped in the tubular (t) system of mechanically skinned rat skeletal muscle fibres to measure SOCE during intracellular Ca^{2+} release. Cytosolic Ca^{2+} transients were simultaneously imaged using the fluorescence of rhod-2. Spatially and temporally resolved images of t system $[Ca^{2+}]$ ($[Ca^{2+}]_{t\text{-}sys}$) allowed estimation of Ca^{2+} entry flux from the rate of decay of $[Ca^{2+}]_{t\text{-}sys}$. Ca^{2+} release was induced pharmacologically to activate SOCE without voltage-dependent contributions to Ca^{2+} flux. Inward Ca^{2+} flux was monotonically dependent on the $[Ca^{2+}]$ gradient, and strongly dependent on the transmembrane potential. The activation of SOCE was controlled locally. It could occur without full Ca^{2+} store depletion and in less than a second after initiation of store depletion. These results indicate that the molecular agonists of SOCE must be evenly distributed throughout the junctional membranes and can activate rapidly. Termination of SOCE required a net increase in $[Ca^{2+}]_{SR}$. Activation and termination of SOCE are also demonstrated, for the first time, during a single event of Ca^{2+} release. At the physiological $[Ca^{2+}]_{t\text{-}sys}$, near 2 mM (relative to t system volume), SOCE flux relative to accessible cytoplasmic volume was at least 18.6 μM s^{-1}, consistent with times of SR refilling of 1–2 min measured in intact muscle fibres.

(Received 19 April 2007; accepted after revision 11 June 2007; first published online 14 June 2007)

Corresponding author B. S. Launikonis: School of Biomedical Sciences, The University of Queensland, Brisbane, Qld, 4072, Australia. Email: b.launikonis@uq.edu.au

Store-operated Ca^{2+} entry (SOCE) is a regulated flow of external Ca^{2+} into cells to refill depleted internal stores (Parekh & Putney, 2005), which occurs in both non-excitable and excitable cells. Given the diverse range of cells for which SOCE is functional it would be reasonable to expect quite different adaptations of this mechanism, tailored around the specific function and structure of the individual cell. For example, the highly specialized skeletal muscle cell regulates changes in cytoplasmic $[Ca^{2+}]$ ($[Ca^{2+}]_c$) of two orders of magnitude within milliseconds (Rome, 2006) in the process known as excitation–contraction (EC) coupling (Melzer *et al.* 1995). Consistent with varying functional needs, EC coupling displays different molecular structures and kinetics even among skeletal muscle cells of different taxa (Di Biase & Franzini-Armstrong, 2005). Changes in $[Ca^{2+}]_c$ in non-excitable cells are slower and occur over much longer periods (Parekh & Putney, 2005). Skeletal muscle and non-excitable cells may well have evolved SOCE with different features, adequate for different demands. For instance, it is reasonable to expect that Ca^{2+} entry in response to store depletion will activate more quickly in skeletal muscle cells than in non-excitable cells.

The structure of the interface of the cell with its exterior should also affect the SOCE mechanisms. Most non-excitable cells are small and compact. In these the endoplasmic reticulum (ER) commands the plasmalemmal store-operated Ca^{2+} (SOC) channel to open upon store depletion, which may require aggregation of receptors or ER translocation (Wu *et al.* 2006; Luik *et al.* 2006; Lewis, 2007). In contrast, skeletal muscle cells are large and elongated. In these cells, the surface membrane consists of a sarcolemma and the tubular (t) system, a network of narrow tubules that invaginate into the cell at regular intervals (Veratti, 1961; Eisenberg, 1983). The large area and close apposition of this membrane system with the Ca^{2+} store (the sarcoplasmic reticulum, or SR) make the t system a chief candidate locus for SOCE.

This paper has online supplemental material.

 DOI: 10.1113/jphysiol.2007.135046

SOCE was indeed shown to be functional at the level of the t system in studies with mechanically skinned skeletal muscle fibres (Launikonis *et al.* 2003). These preparations, which have the sarcolemma mechanically removed causing the t system to reseal, maintain the normal physiological function (including an action potential-induced Ca^{2+} release from SR at a normal rate; Posterino & Lamb, 2003; Launikonis *et al.* 2006). In addition to identifying the t system membrane as the locus of Ca^{2+} entry, the studies with mechanically skinned fibres exhibited a singular advantage: the resealing of t tubules after skinning results in formation of a finite pool of extracellular Ca^{2+}.

A method of imaging Ca^{2+} in the t system of skinned fibres was developed in the Stephenson laboratory more than a decade ago (Stephenson & Lamb, 1993; Lamb *et al.* 1995). Following the identification of SOCE in skeletal muscle (Kurebayashi & Ogawa, 2001), this method was modified to study SOCE by trapping the low affinity Ca^{2+}-sensitive dye, fluo-5N, in the t system (Launikonis *et al.* 2003). This study showed that the resealed t system could be depleted of Ca^{2+} in less than 30 s following application of caffeine and that depletion failed when the skinned fibres were exposed to high intracellular $[Ca^{2+}]$, a treatment that disrupts the functional coupling between SR and t system (Lamb *et al.* 1995). These experiments thus confirmed the presence of the store-operated pathway in the t system membrane and validated its assessment from changes in Ca^{2+}-dependent fluorescence in the resealed t system (Launikonis *et al.* 2003).

Brotto and colleagues also used a non-ratiometric dye trapped in the t system of skinned fibres in attempts to measure SOCE during SR Ca^{2+} release. In contrast to the results of Launikonis *et al.* (2003), they reported a t system fluorescence signal that declined only slowly over a period of more than 10 min upon caffeine application (Zhao *et al.* 2005, 2006; Hirata *et al.* 2006).

To improve quantification of the decay of $[Ca^{2+}]$ in the t system ($[Ca^{2+}]_{t\text{-}sys}$) as a measure of SOCE during intracellular Ca^{2+} release, we used a novel technique to image $[Ca^{2+}]$ inside the t system, shifted excitation and emission ratioing of fluorescence, or SEER (Launikonis *et al.* 2005). SEER improved the quantification because it is ratiometric and has greater sensitivity than previous methods. Additionally, it could be used simultaneously with the cytoplasmic Ca^{2+} indicator rhod-2.

This combination of techniques in skinned fibres allowed for: (i) control of the composition of the t system lumen and cytoplasmic environment; (ii) recording of $[Ca^{2+}]$ simultaneously in t system and cytoplasm; and (iii) reliably estimating the $[Ca^{2+}]_{SR}$ load by extrapolation from similar experiments where $[Ca^{2+}]_{SR}$ is measured (experiments communicated here and by Fryer & Stephenson, 1996; Herrmann-Frank *et al.* 1999; Launikonis *et al.* 2005, 2006).

Voltage-dependent currents were avoided by directly activating the Ca^{2+} release channel/ryanodine receptor (RyR) of the SR by pharmacological means – rather than by depolarization of the plasma membrane – in solutions that maintain a constant membrane potential (Lamb & Stephenson, 1994). Furthermore, $[Ca^{2+}]_c$ was buffered with EGTA and BAPTA to restrict the uptake of cytoplasmic Ca^{2+} by the t system. The decay in $[Ca^{2+}]_{t\text{-}sys}$ during Ca^{2+} release observed this way was found to be largely due to SOCE. The measurable rate of change of $[Ca^{2+}]_{t\text{-}sys}$ thus provides a direct quantification of store-dependent Ca^{2+} influx simultaneously with intracellular Ca^{2+} release.

Methods

All experimental methods were approved by the Institutional Animal Care and Use Committee at Rush University. Sprague–Dawley rats (250–300 g) were killed by CO_2 asphyxiation and the extensor digitorum longus (EDL) muscles were rapidly excised. Muscles were then placed in a Petri dish under paraffin oil above a layer of Sylgard.

The method of trapping fluorescent dye in the sealed t system has been described (Lamb *et al.* 1995; Launikonis *et al.* 2003; Launikonis & Stephenson, 2004). Briefly, small bundles of fibres were isolated and exposed to a 'dye solution' while still intact. Individual fibres were then isolated and mechanically skinned. Skinned fibres were transferred to a custom built experimental chamber with a coverslip bottom, where they were bathed in an 'internal solution'.

Solutions

The dye-containing solution applied before skinning of rat fibres contained (mM): NaCl, 145; KCl, 3; $CaCl_2$, 2.5; $MgCl_2$, 2; mag-indo-1 salt, 10; and Hepes 10 (pH adjusted to 7.4 with NaOH). The standard internal solutions are shown in Table 1. High $[K^+]$ solutions kept the sealed t system polarized and high $[Na^+]$ depolarized it (Lamb & Stephenson, 1994). Reference solutions were used to load SR and t system with Ca^{2+} and to preequilibrate the preparations to appropriate buffering and membrane potential conditions before Ca^{2+} release. Solutions with caffeine and low Mg^{2+} solution were designed to induce SR Ca^{2+} release (Launikonis & Stephenson, 2000; Lamb *et al.* 2001).

Confocal imaging

Imaging was done as described in Launikonis *et al.* (2005). Briefly, the experimental chamber was placed above the water immersion objective (40×, NA 1.2) of the confocal

Table 1. Composition of internal solutions

Solution	K^+	Na^+	Ca^{2+}	Mg^{2+}	EGTA	BAPTA	Caffeine
Reference–0 Ca^{2+}	100	30	0	0.65	1	0	0
Reference–100 Ca^{2+}	100	30	0.0001	0.65	1	0	0
Reference–800 Ca^{2+}	100	30	0.0008	0.65	1	0	0
Reference–0 Ca^{2+}–BAPTA	100	30	0	0.65	0	5	0
Reference–Na–0 Ca^{2+}	0	130	0	0.65	1	0	0
Reference–Na–800 Ca^{2+}	0	130	0.0008	0.65	1	0	0
Low Mg^{2+}	100	30	0	0.01	1	0	0
Caffeine	100	30	0	0.01	1	0	30
Low Mg^{2+}–BAPTA	100	30	0	0.01	0	5	0
Caffeine–BAPTA	100	30	0	0.01	0	5	30
Caffeine–depol	0	130	0	0.01	1	0	30

All concentrations are in mM. Additionally, solutions contained (mM): glutamate, 100; creatine phosphate, 10; ATP, 5; Hepes, 10; rhod-2, 0.1. Mg^{2+} was added as $MgCl_2$ and Ca^{2+} was added as $CaCl_2$. Note that 'Mg^{2+}' and 'Ca^{2+}' refer to concentrations of free divalents in solution and that total concentrations of Mg and Ca added were much higher. Osmolality was adjusted to 290 ± 10 mosmol kg^{-1} with sucrose and pH was set to 7.1 with KOH or NaOH. BTS (SIGMA-Aldrich Co, St Louis, MO, USA; *n*-benzyl-*p*-toluene sulphonamide; 50 μM) was added to all solutions to suppress contraction (Cheung *et al.* 2002). 2-Aminoethyl diphenyl borate (2-APB; 0.1 mM; Sigma-Aldrich) was added to solutions as required from a 100 mM stock in DMSO.

laser scanning system (TCS SP2, Leica Microsystems, Exton, PA, USA). Simultaneous acquisition of three images (F_1, F_2 and F_3) was achieved by line-interleaving of three excitation wavelengths (351, 364 and 543 nm) while collecting emitted light in three emission ranges (390–440 nm, 465–535 nm, and 562–666 nm).

Calibration of $[Ca^{2+}]_{t\text{-}sys}$

SEER of mag-indo can be used to image $[Ca^{2+}]$ inside cellular organelles, as previously demonstrated in SR (Launikonis *et al.* 2005). Equation (1) (Grynkiewicz *et al.* 1985), with parameters defined in Launikonis *et al.* (2005), was assumed to describe the relationship between R and $[Ca^{2+}]_{t\text{-}sys}$:

$$[Ca^{2+}](x, y) = \gamma K_D[R(x, y) - R_{min}]/[R_{max} - R(x, y)] \quad (1)$$

To determine the $[Ca^{2+}]$ inside the t system, dye-loaded preparations were bathed in calibration solutions, which were a standard potassium glutamate internal saline with 0.65 mM Mg^{2+}, 5 μM A23187 (Sigma Aldrich) and 5 μM ionomycin. $[Ca^{2+}]_c$ (0–1 mM) was buffered by 15 mM EGTA or nitrilotriacetate in the appropriate range.

$[Ca^{2+}]_c$ higher than 1 mM in the bathing solution appeared to cause loss of dye from the preparation, a problem also found in calibrations of mag-indo-1 (fluorscent dye from molecular probes) inside the SR (Launikonis *et al.* 2005). To circumvent this problem R_{max} was determined in conditions that promoted heavy loading of Ca^{2+} into the t system, namely an internal solution with 800 nM Ca^{2+} and all K^+ replaced with Na^+ to depolarize the t system. R_{max} was thus determined to be 4.82 ± 0.04 in three fibres. This value was close to the one found by a similar approach in calibrations of mag-indo-1 inside SR in frog muscle fibres (Launikonis *et al.* 2005). While it is not certain that the concentration reached inside the organelle under these conditions is sufficient to saturate the dye, a nearly identical value of R_{max}, 4.98 ± 0.05 ($n = 3$), was found by the same method for indo-1, a dye that is nearly identical optically, but has a roughly 100 times greater affinity for Ca^{2+}. Fitting eqn (1) to all R *versus* $[Ca^{2+}]$ data, with R_{max} set to 4.82, yielded the following values for the other parameters: $\gamma K_D = 0.615$ mM and $R_{min} = 0.45$. This prediction of R_{min} was later confirmed experimentally. When applying the release-inducing low Mg^{2+}–BAPTA to freshly skinned preparations, R in the t system could not fall below 0.45 when inducing store-operated Ca^{2+} depletion (three fibres), confirming this as the R_{min} value.

$[Ca^{2+}]$ in two compartments during release

Simultaneous SEER and rhod-2 images provided spatially and temporally resolved measures of $[Ca^{2+}]_{t\text{-}sys}$ and $[Ca^{2+}]_c$ during Ca^{2+} release. Ca^{2+} was released under conditions leading to known total SR calcium, $[Ca^{2+}]_{SR}$ and cytoplasmic transients (Fryer & Stephenson, 1996; Launikonis & Stephenson, 2000; Launikonis *et al.* 2005, 2006). Thus, even though we only imaged cytoplasmic and t system $[Ca^{2+}]$ during release, we could estimate that within the SR with some confidence.

SOCE was quantified during Ca^{2+} release induced by five different solutions (detailed in Table 1). The first was 'low Mg^{2+}', containing 10 μM Mg^{2+}, and 1 mM EGTA for nominally 0 $[Ca^{2+}]$. This solution elicited Ca^{2+} release that was brief and ceased during imaging, leading to immediate reuptake by the SR (Launikonis *et al.* 2006).

Thus, this condition allowed for measurement of transmembrane Ca^{2+} movements during a complete sequence of SR depletion (which was partial) and recovery. A second condition 'low Mg^{2+}–BAPTA', suppressed the cytosolic Ca^{2+} transient. Two other conditions added 30 mM caffeine to the respective low Mg^{2+} solutions. This enhanced release of SR Ca^{2+} and kept the RyR in a highly active state, preventing any net reuptake of Ca^{2+} into the SR. In another series of experiments Na^+ replaced all K^+ in the solution 'caffeine–depol', to depolarize the sealed t system. This was in contrast to all the K^+-based solutions, which were designed to keep the t system polarized (Lamb & Stephenson, 1994).

It should be noted that in the mammal, Ca^{2+} release via direct activation of the RyR is faster in the presence of BAPTA than EGTA. We understand this as a consequence of rapid Ca^{2+} chelation by BAPTA, which suppresses Ca^{2+}-dependent inactivation and has no inhibitory effects, in agreement with the reported absence of Ca^{2+}-induced Ca^{2+} release in mammalian muscles (Shirokova *et al.* 1996, 1998; Launikonis & Stephenson, 2000), presumably due to lack of the RyR3 isoform (Zhou *et al.* 2004; Pouvreau *et al.* 2007).

Reference solutions with either 100 or 800 nM Ca^{2+} and Reference–Na–800 Ca^{2+} (Table 1) were used to load Ca^{2+} into the t system and SR. There is no precedent study setting conditions for loading Ca^{2+} to appropriate levels in t system and SR of skinned fibres. So approaches which allowed appropriate levels in $[Ca^{2+}]_{t\text{-}sys}$ for experiments to be reached while loading SR close to endogeneous levels were developed. In many cases preparations were left in the order of 5–15 min in Reference–100 Ca^{2+}. We expect this loading protocol to cause Ca^{2+} in SR to plateau not much beyond endogeneous levels (Launikonis *et al.* 2005). In some experiments 800 nM Ca^{2+} was used to load Ca^{2+} for periods not more than 30 s to avoid overload of SR and reduce the time required to load Ca^{2+} into the t system. During the course of experiments it was found that Reference–Na–800 Ca^{2+} loaded the t system at a faster rate than Reference–800 Ca^{2+}. This probably reflects the greater capacity of t system Ca^{2+}-ATPase to translocate Ca^{2+} in the absence of an electrical gradient. Therefore, Reference–Na–800 Ca^{2+} was the preferred Ca^{2+} loading solution. In most cases we expect SR was loaded with Ca^{2+} at or slightly above its endogeneous level but not 'heavily' loaded (i.e. close to full; Launikonis & Stephenson, 2000). This is also evident from the moderate time courses of the cytoplasmic Ca^{2+} transients in the presence of 1 mM EGTA (Figs 4, 7 and 8). However, the final $[Ca^{2+}]_{SR}$ is not precisely known.

Analysis of changes in $[Ca^{2+}]_{t\text{-}sys}$

As the sealed t system is a closed, finite compartment, any change in $[Ca^{2+}]_{t\text{-}sys}$ must be due to Ca^{2+} flux across the membrane (Almers *et al.* 1981; Friedrich *et al.* 2001) or changes in the volume of the compartment. In the following we neglect the changes in volume (see below; Launikonis & Stephenson, 2004), and assume that J_{Ca}, the net Ca^{2+} flux across the t system membrane, is proportional to the rate of change, $d[Ca^{2+}]_{t\text{-}sys}/dt$.

When expressed relative to the volume of the t system, the total calcium concentration of the organelle is probably in the tens of millimolar range (Hidalgo *et al.* 1986; Owen *et al.* 1997), with most calcium presumably bound to low-affinity sites on membrane proteins. Therefore the net rate of change of total calcium concentration due to entry to the cytosol, $d[\text{calcium}]_c/dt$, should be equal to $Ad[Ca^{2+}]_{t\text{-}sys}/dt$, where A is the product of the fractional volume of the t system within the intact fibre ($\text{t-sys}_{vol} = 0.014$; Launikonis & Stephenson, 2002*a*) and a factor representing the ratio between bound and free Ca^{2+} in the t system (β), which is expected to be roughly constant but will remain unknown.

We should point out that in the text we refer to Ca^{2+} current across the sealed t system inferred from net loss of $[Ca^{2+}]_{t\text{-}sys}$ as 'Ca^{2+} influx' or 'Ca^{2+} entry', for consistency with terms describing Ca^{2+} movements in intact muscle fibres.

SEER imaging of Ca^{2+} inside the t system

Figure 1 shows confocal *xy* images of mag-indo-1 in the t system of a mechanically skinned rat EDL fibre. The fibre had been bathed in a physiological solution containing mag-indo-1 while still intact and then mechanically skinned to trap the dye in the t system, as previously described (Lamb *et al.* 1995; Launikonis *et al.* 2003; Launikonis & Stephenson, 2004). Figure 1*A* and *B* are images F_1 and F_2, respectively, of a fibre bathed in low Mg^{2+}. The images show two t tubules per sarcomere and infrequent longitudinal connections, which were originally described by Veratti (1961). Note that longitudinal structures appear across the long gap between the t tubules, crossing the M line, and run in series.

The ratio (R) of F_1 and F_2 is shown in Fig. 1*C*, only in 'well-stained' regions, defined as those in the upper quartile of the distribution of the dye (calculated as described by Launikonis *et al.* 2005). Raw ratioing of F_1 and F_2 (not shown) does not exhibit a clear arrangement of two t tubules per sarcomere. The dye-based restriction of the image clearly recovers the double t tubular structure. Results presented below (Figs 4, 5, 6, 7 and 8) will show that R computed this way monitors t system $[Ca^{2+}]$ ($[Ca^{2+}]_{t\text{-}sys}$).

Furthermore, we can calculate the concentration of mag-indo-1 in the t system, $[\text{mag-indo-1}]_{t\text{-}sys}$, in this image (Launikonis *et al.* 2005). In Fig. 1, $[\text{mag-indo-1}]_{t\text{-}sys}$ is 12.2 μM. This is much less than the 10 mM mag-indo-1

present in the dye solution applied to the intact fibre, probably due to a combination of factors, including dilution of mag-indo-1 in the normal extracellular fluid surrounding the intact fibre, some 'squeezing-out' of the dye that entered the intact t system during the skinning process, and slow extrusion from the t system by anion transporters (Launikonis & Stephenson, 2002*b*, 2004). $[\text{mag-indo-1}]_{\text{t-sys}}$ was always in the low micromolar range, and therefore no major Ca^{2+} buffering effects should be expected from the monitoring dye.

Analysis of confocal images

All imaging in this study was performed in *xy* mode, in most cases at 0.2324 μm pixel distance and 1.25 ms line interval. *xy* scanning lent itself to a method of image analysis illustrated in Fig. 2. The scanning line, defining the variable x, was transversal to the fibre axis. *xy* imaging provided information in two dimensions of space and in a temporal dimension as well, along the y axis. The temporal evolution of $[Ca^{2+}]_{\text{t-sys}}$ and $[Ca^{2+}]_{\text{c}}$ could be derived by averaging, respectively, $R(xy)$ or $F_3(xy)$ over x within the borders of the preparation, to obtain a function ($R(y)$ or $F_3(y)$) of y that mapped proportionally to elapsed time. The correspondence factor between t and y, 16.1 ms per μm, is determined by the group scanning speed (3.75 ms per line in each of 3 images, and pixel distance). For the approach to be valid, the fibre must be homogeneous along the y axis, which usually can be decided by inspection of the *xy* image at rest. Uniformity is considered reasonable when changes of $R(y)$ in the resting fibre are minor relative to the magnitude and rate of the dynamic changes $R(y(t)) = G(t)$ of interest during stimulated release. For instance, in the case of Fig. 2 the sarcomeric structure imposes an oscillatory pattern of period *ca* 2 μm or 32.2 ms and amplitude ~20% peak-to-peak. Other minor irregularities add to the variance of $R(y)$. This degree of uniformity is sufficient if the goal is to reveal greater, faster or longer-lasting components in $G(t)$. The events illustrated in Figs 4, 5, 6, 7 and 8 clearly satisfy this criterion. Figure 2 illustrates a degree of homogeneity that is suitable.

In experiments represented in Figs 4, 5, 6, 7 and 8 R refers to the ratio of F_1/F_2 of mag-indo-1 in the t system and the normalization of cytoplasmic rhod-2 fluorescence is represented as $F_3/F_{3,0}$. The reference (F_0) for normalization of rhod-2 fluorescence was $F_3(y)$ within the borders of the preparation under resting conditions immediately prior to exposure of the preparation to release-inducing solution. The F_0 value may not represent the minimum F_3 value in the F_3 image (fluorescence can be lower in the surrounding bathing solution) in Figs 4, 5, 6, 7 and 8. In Fig. 3, a different combination of dyes was used. R refers to the ratio F_1/F_2 of indo-5F in the cytoplasm and $F_3/F_{3,0}$ represents normalized value of fluo-3 fluorescence in the t system to that under resting conditions.

Volume changes in the sealed t system during Ca^{2+} release

In this work store-dependent Ca^{2+} flux is assessed from the net change in $[Ca^{2+}]_{\text{t-sys}}$ following Ca^{2+} release. Any change in volume of the t system due to water flux during Ca^{2+} release will confound our derivation of Ca^{2+} entry. Although the volume of the sealed t system of rat skeletal muscle varies little during osmotic stress (Launikonis & Stephenson, 2004), it was important to check whether this was the case during Ca^{2+} release. For this purpose fluo-3 was trapped in the t system of rat skeletal muscle. Because fluorescence of fluo-3 is at saturation values, its changes only reflect the evolution of ionic strength, and can be used to derive change in volume (Launikonis & Stephenson, 2004).

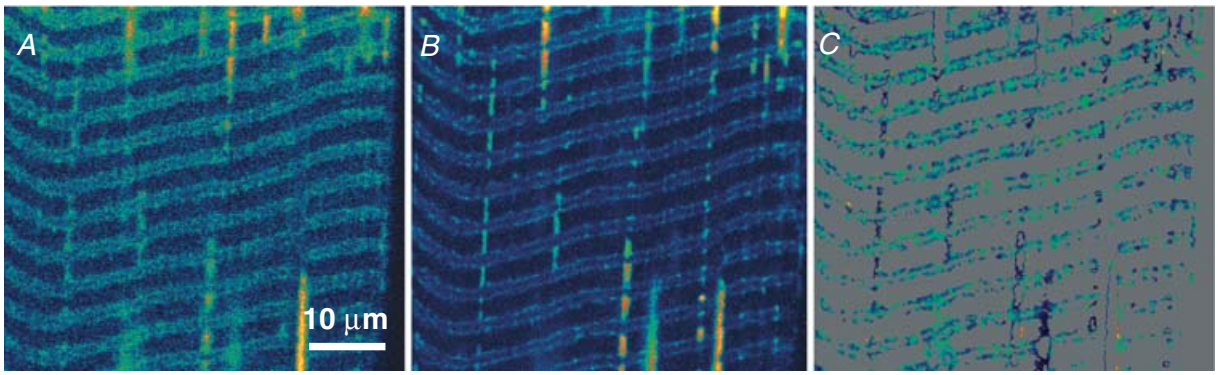

Figure 1. SEER imaging of mag-indo-1 inside the sealed t system of a rat skinned fibre
A, image of fluorescence F_1 (acquired as defined in Methods); *B*, image F_2; *C*, $R = F_1/F_2$, spatially restricted to the two upper quartiles of the dye distribution (Launikonis *et al.* 2005). Fibre was bathed in low Mg^{2+}. Image-averaged R was 1.82, corresponding to a $[Ca^{2+}]_{\text{t-sys}}$ of 0.28 mM. Average dye concentration in the well-stained region was 12.2 μM. (ID: 101805c_#11.)

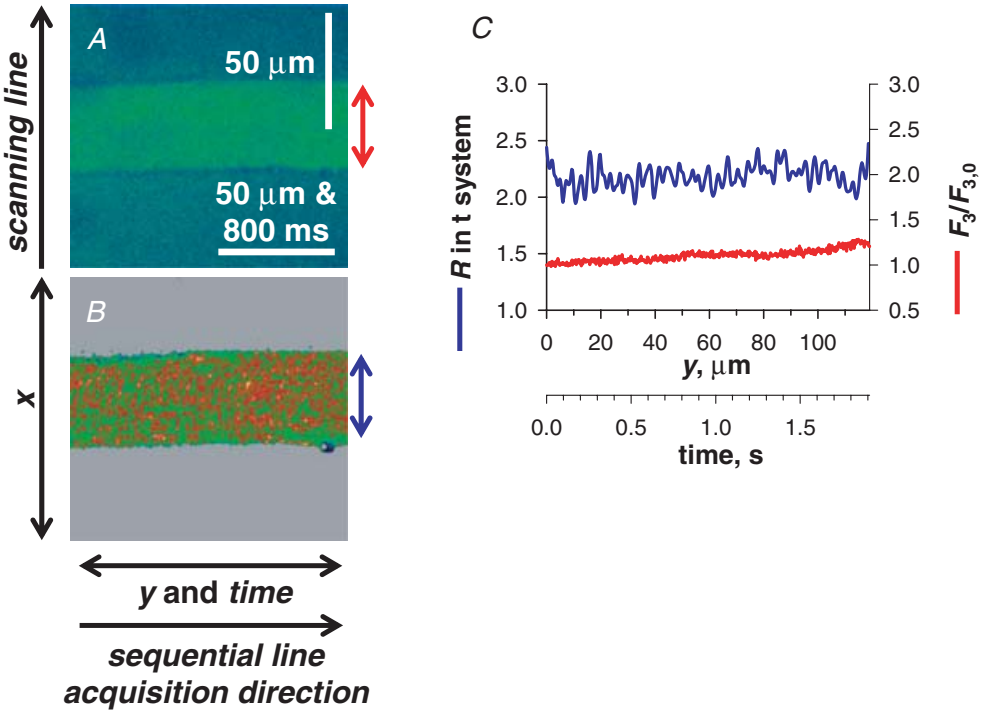

Figure 2. Image acquisition and analysis
A, F_3 image. *B*, simultaneously acquired *R* in t system. The scanning line was transversal to the fibre axis, *x*, with each line (512 total) sequentially acquired along the longitudinal axis of the fibre, *y*. *C*, spatially averaged values of F_3 and *R* from within the borders of the preparation, as indicated by the double arrows of corresponding colour. Note that *y* maps proportionally to time. (ID: 072805f_s025_z007.)

The t system and SR were initially loaded with Ca^{2+} in a reference solution containing 800 nM Ca^{2+}. The preparation was then exposed to a low Mg^{2+} solution containing 100 μM indo-5F, which induced Ca^{2+} release and allowed us to image the Ca^{2+} transient. As shown in Fig. 3, after an artifact caused by the change in solution the fluo-3 fluorescence decreased at a constant rate, both during and after Ca^{2+} release. This steady decrease is due to bleaching and slow loss of dye from the sealed t system (Launikonis & Stephenson, 2002*b*, 2004). This result was obtained on all three fibres examined. The result indicates that there were no significant changes in volume of the t system specifically associated with Ca^{2+} release.

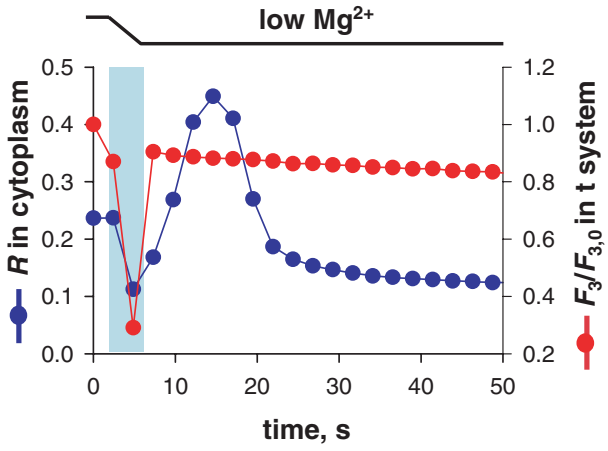

Figure 3. Ca^{2+} release is not associated with a change in volume of the sealed t system
Image-averaged fluorescence of cytoplasmic indo-5F (blue) and of fluo-3 trapped in t system (red), *versus* time. At between 3 and 6 s (light blue bar), the bathing solution was changed from reference to the release-inducing low Mg^{2+}. Fluorescence of fluo-3 in the t system, which presumably corresponds to a fully Ca^{2+}-saturated level, decays throughout at a steady low rate. (ID: 012306a_s008.)

Quenching of fluorescence by caffeine

Caffeine at concentrations greater than 10 mM can quench fluorescence signals of Ca^{2+} sensitive dyes, inducing a shift in the R_{min} and R_{max} that has been demonstrated with indo dyes (Muschol *et al.* 1999; McKemy *et al.* 2000). To quantify the effect in these preparations, R_{max} and R_{min} were determined in the presence of 30 mM caffeine.

R_{min} was determined by allowing $[Ca^{2+}]_{t\text{-}sys}$ to decrease in the presence of caffeine–BAPTA solution. The average thus found in three freshly skinned preparations, 0.73 ± 0.05 ($n = 3$), is significantly larger than the value (0.45) determined in the same way using low Mg^{2+}–BAPTA as stimulus for Ca^{2+} release.

R_{max} was determined as the maximum reached early when exposing the preparations to 30 mM caffeine and

5 mM BAPTA. This solution causes a rapid release of SR Ca^{2+} (Launikonis & Stephenson, 2000) which is accumulated rapidly by the t system (data not shown). The maximum R was 5.5 ± 0.07 in three preparations.

Results

This section includes images of the evolution of $[Ca^{2+}]$ within the t system during SR Ca^{2+} depletion, quantified to derive Ca^{2+} flux, with simultaneously recorded images of $[Ca^{2+}]_c$ at both the normal resting membrane potential and in the chronically depolarized cell. $[Ca^{2+}]_{t\text{-}sys}$ is measured by SEER and calibrated *in situ*. Two types of stimuli were used, leading to Ca^{2+} release of different duration and extent in conjunction with two cytosolic buffers, to exert different degrees of control of $[Ca^{2+}]_c$.

SOCE during store depletion and recovery

Simultaneously acquired cytoplasmic rhod-2 and t system SEER images are shown in Fig. 4. A summary in Fig. 4*C* of the temporal evolution of $[Ca^{2+}]_{t\text{-}sys}$ and $[Ca^{2+}]_c$ was derived by averaging over x within the borders of the preparation, to obtain a function of y that mapped proportionally to elapsed time (see Methods and Fig. 2).

Changing the internal solution from reference with 100 nM Ca^{2+} and 0.65 mM Mg^{2+} to low Mg^{2+} (a nominally Ca^{2+}-free solution with 1 mM EGTA and 10 μM Mg^{2+}) caused the release of SR Ca^{2+}. The drop in internal solution $[Ca^{2+}]$ is shown by the reduction in F_3 fluorescence intensity around the preparation. The spatial progression of Ca^{2+} release (probably timed by diffusion of Mg^{2+} away from the fibre) results in a V-shaped Ca^{2+} transient in image *A* at 6 s and in narrowing of the area of low $[Ca^{2+}]$ surrounding the fibre, as released Ca^{2+} diffuses into this area. Note that the membrane potential was held at its resting value across the t system throughout the duration of this experiment (Lamb & Stephenson, 1994).

During the initial rise of the Ca^{2+} transient, $[Ca^{2+}]_{t\text{-}sys}$ increased (image *B* at 6 s). Plasma membrane Ca^{2+}-ATPase and Na^+–Ca^{2+} exchanger have both been shown to colocalize with the dihydropyridine receptor at the junctional membrane domain of the t system (Sacchetto *et al.* 1996), making translocation of Ca^{2+} by these proteins the most likely explanation for the increase in $[Ca^{2+}]_{t\text{-}sys}$ (Hidalgo *et al.* 1986, 1991; Donoso *et al.* 1995). Later, prior to the peak of the Ca^{2+} transient (*B* at 6 s; see also graph in Fig. 4*C*), there was a sharp reversal of the direction of change in $[Ca^{2+}]_{t\text{-}sys}$, i.e. in the sign of net t system flux, which became negative. Later, at about 10 s, there was another reversal in flux, indicating net Ca^{2+} entry to the t system. This pattern of Ca^{2+} movements in the presence of low Mg^{2+} was observed in five fibres.

Using mag-indo-1 in the SR, we previously showed that the SR starts to take up Ca^{2+} and recover from depletion at the time of RyR closure (Fig. 4 in Launikonis *et al.* 2006). Therefore the concomitant inversion in sign of the rate of change in $[Ca^{2+}]_{t\text{-}sys}$ (which as explained in Methods we interpret as change of net flux) observed here between 11 and 13 s is consistent with reduction of a store-operated inward component of this flux below the level of a presumably small efflux, and validates measurement of $[Ca^{2+}]_{t\text{-}sys}$ as a monitor of SOCE.

Attempts were made to block SOCE with the commonly used agent 2-APB. It was found that low Mg^{2+} was no longer able to elicit Ca^{2+} release from SR when in the presence of 0.1 mM 2-APB. This result was observed in three preparations. There was no effect of the addition of 0.1% DMSO (2-APB vehicle) to low Mg^{2+} solution alone on Ca^{2+} release. Therefore these experiments were abandoned. It is known that 2-APB interacts with a number of proteins, including the inositol trisphosphate receptor (Parekh & Putney, 2005), and therefore an interaction with RyR1 would not be surprising.

SOCE with suppressed changes in $[Ca^{2+}]_c$

In the above experiment, the signal from cytosolic rhod-2 demonstrates a significant increase in $[Ca^{2+}]_c$ during release in the presence of 1 mM EGTA (Fig. 4). An exploration of the effects of $[Ca^{2+}]_c$ was called for because its increase could directly affect SOCE (Hoth & Penner, 1993; Zweifach & Lewis, 1995) and should promote Ca^{2+} uptake by the t system, thus complicating the evaluation of SOCE through net flux. To evaluate these points, we performed similar release experiments as those above, with the addition of 5 mM BAPTA to the release-inducing solution.

R and rhod-2 images are shown in Fig. 5*A* and *B* for a fibre exposed to low Mg^{2+}–BAPTA. Immediately prior to this exposure, the preparation was passed through reference with 800 nM Ca^{2+} to increase $[Ca^{2+}]_{t\text{-}sys}$ and then equilibrated to a reference solution with BAPTA and no added calcium. R and F_3 averaged over x are plotted *versus* y or time in Fig. 5*C*. $[Ca^{2+}]_{t\text{-}sys}$ was uniform throughout the fibre prior to release (see online supplemental material). A small cytosolic Ca^{2+} transient, of magnitude $0.1F_0$, was induced by the stimulus in the presence of BAPTA. Probably because the transient was small, the decay in $[Ca^{2+}]_{t\text{-}sys}$ started without any preceding uptake of Ca^{2+}. This result was obtained on the two fibres tested in this manner. Note also that a V-shaped spatiotemporal pattern of Ca^{2+} release from the SR, similar to that in Fig. 4, should have occurred as Mg^{2+} diffused away from the preparation. This is not reported by the cytoplasmic rhod-2 due to the presence of BAPTA (Fig. 5).

The inset of Fig. 5*C* plots the evolution of *R* restricted to the central or peripheral regions of the preparation, for the first 1.9 s after immersion in low Mg^{2+}–BAPTA. Decay is faster in the periphery, starting in less than 1 s following introduction of low Mg^{2+}–BAPTA, which suggests that SOCE is rapidly activated and determined by depletion at the local level.

Similar experiments were carried out using caffeine–BAPTA, following the same protocol as in Fig. 5. A decay of $[Ca^{2+}]_{t\text{-}sys}$ without recovery, starting within 1–3 s of immersion in caffeine–BAPTA was observed in four preparations. An example is shown in Fig. 6. Note that 15 s in reference solution with BAPTA and 0 Ca did not cause activation of SOCE. Also, there was

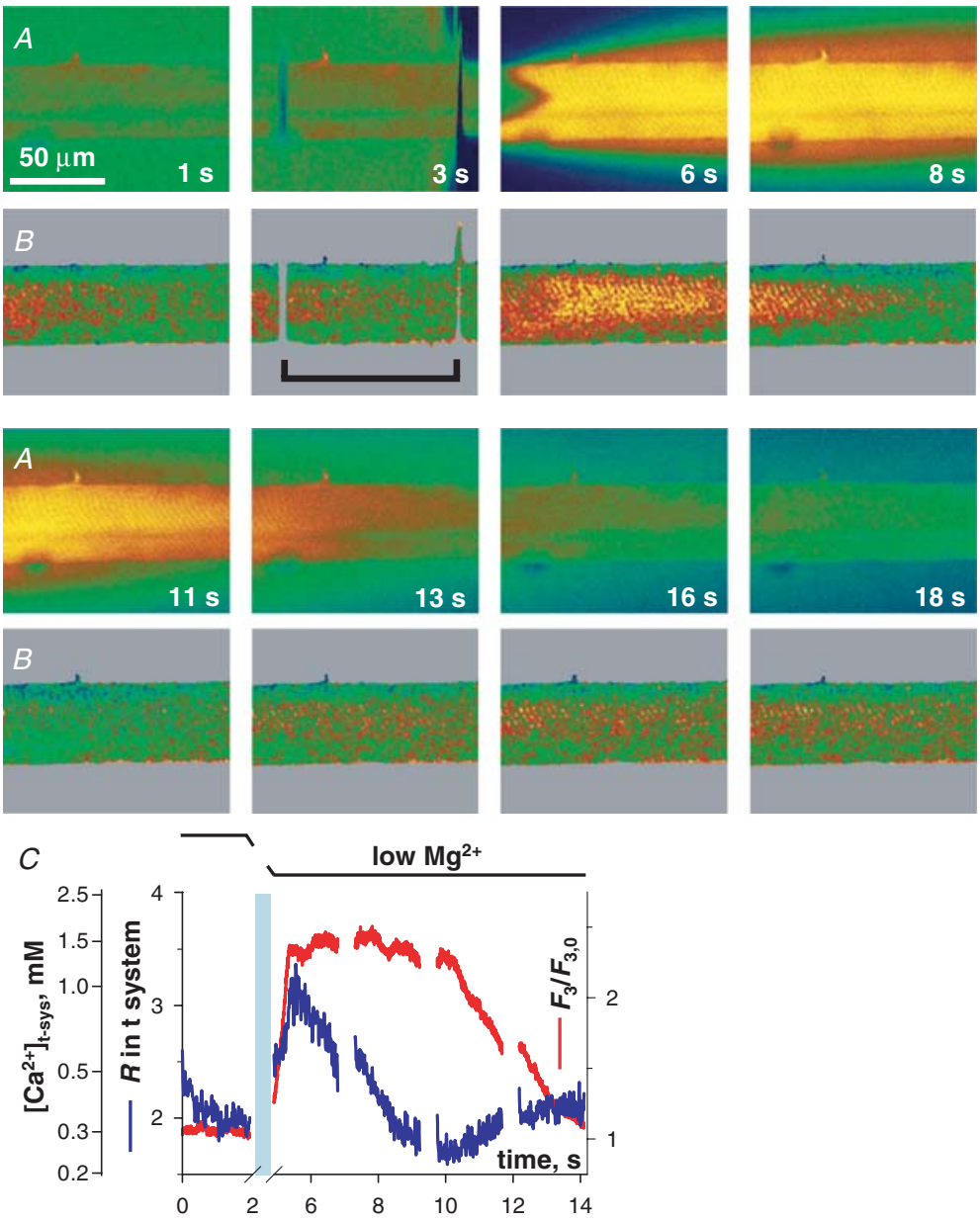

Figure 4. SOCE during Ca^{2+} release and removal
A, selected images of fluorescence F_3 of cytosolic rhod-2 and *B*, ratio *R* of fluorescence images F_1 and F_2 of mag-indo-1 in the t system, simultaneously acquired while applying the release-inducing low Mg^{2+} solution. *C*, spatially averaged values of F_3 (normalized by resting value $F_{3,0}$, red) and *R* (blue) *versus* elapsed time (which maps to the abscissa of *x*–*y* scans as described in Methods). The interval of solution change is indicated by the black bracket in image *B* at 3 s, and by the light blue bar in *C*, where fluorescence and ratio plots were omitted during solution change. (ID: 072005b_s013.)

a small increase in $[Ca^{2+}]_{t\text{-}sys}$ preceding the increase in F_3. This suggests that the t system devices for Ca^{2+} uptake respond to a local rise in $[Ca^{2+}]$ in the microdomain of the 'couplon' (Stern *et al.* 1997) before the global $[Ca^{2+}]$ increase is reflected in changes in F_3.

In Fig. 6 the effect of caffeine quenching of mag-indo-1 fluorescence from the t system can be observed as an abrupt upward shift in R at the point of caffeine introduction to the bathing solution (Fig. 6*B* and *C*). The shift constitutes a change in dye properties, which required a different calibration in the presence of caffeine (McKemy *et al.* 2000). In Fig. 6*D* the average $[Ca^{2+}]_{t\text{-}sys}$ in x has been plotted against y or time. The continuity of $[Ca^{2+}]_{t\text{-}sys}$ is maintained, indicating that parameters used to determine $[Ca^{2+}]_{t\text{-}sys}$ from R in either the presence or the absence of caffeine were adequate (see Methods).

Following activation of SOCE, $[Ca^{2+}]_{t\text{-}sys}$ did not significantly recover in caffeine–BAPTA (Fig. 6). This time course is consistent with the lack of recovery of $[Ca^{2+}]_{SR}$ during continued caffeine exposure (Launikonis & Stephenson, 2000), again indicating that the inward flux of Ca^{2+} under the conditions described is largely store-operated. Thus, only an exit flux from the t system is observed in low Mg^{2+}–BAPTA (Fig. 5) and in caffeine–BAPTA (Fig. 6) if SR is not heavily loaded with Ca^{2+}. In conclusion, SOCE depletes the sealed t system of Ca^{2+} in a few seconds when $[Ca^{2+}]_c$ is kept low.

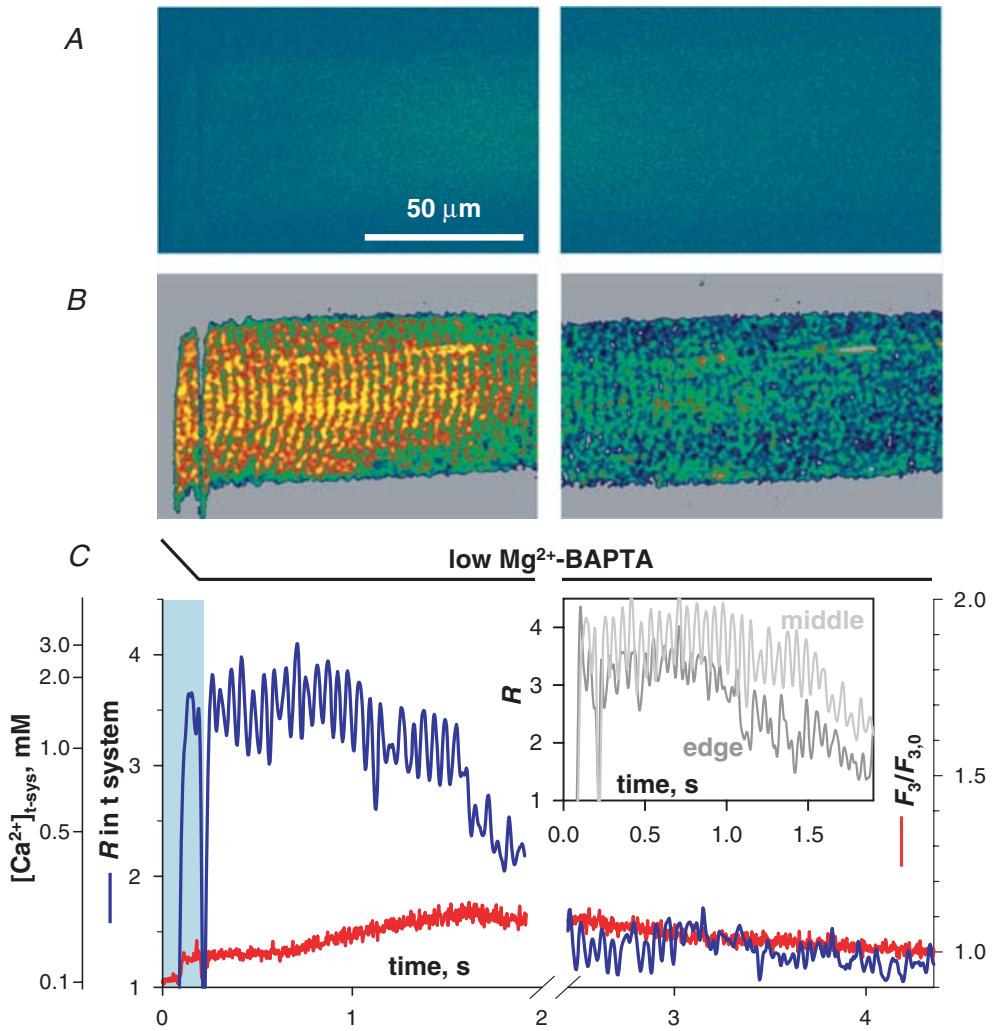

Figure 5. SOCE with suppressed change in $[Ca^{2+}]_c$
A, F_3 and *B*, R in t system, acquired while changing from a solution with 5 mM BAPTA, 0 Ca and 0.65 mM Mg^{2+} to release-inducing low Mg^{2+}–BAPTA. *C*, spatially averaged $F_3/F_{3,0}$ (red) and R (blue) *versus* elapsed time, which directly correspond to time and y axis in *A* and *B*. Inset, average R in central 40 μm ('middle') and 30 μm slice starting at the lower edge ('edge') of the fibre image. Note the periodic pattern of $[Ca^{2+}]_{t\text{-}sys}$ in *C*, which results from the regular placement of t-tubules along the fibre. Other details as in Fig. 4. (ID: 072805f_s012.)

SOCE and membrane potential

To examine the effect of t system membrane potential on the store-operated Ca^{2+} flux, preparations were exposed to K^+- or Na^+-based caffeine solutions in the presence of 1 mM EGTA. An internal solution with only Na^+ will chronically depolarize the t system and a K^+-based internal solution with some Na^+ will activate the t system Na^+-pump and allow the normal $[K^+]$ and $[Na^+]$ gradients to be reestablished across the t system, resulting in a close to normal resting potential (Lamb & Stephenson, 1990, 1994). To assure and ascertain Ca^{2+} store depletion under both conditions of membrane potential, 30 mM caffeine and 1 mM EGTA were used in the solution. Indeed, caffeine facilitates SR Ca^{2+} release under a wide range of conditions and prevents net Ca^{2+} uptake by the SR (Herrmann-Frank *et al.* 1999), while 1 mM EGTA buffers released Ca^{2+} while not hindering the observation of the cytoplasmic Ca^{2+} transient, thus providing an unambiguous indicator of Ca^{2+} release, which can in turn be used to assess depletion.

The evolution of $[Ca^{2+}]_{t\text{-}sys}$ upon caffeine stimulation in a K^+-based glutamate solution is illustrated in Fig. 7. Prior to caffeine, the fibre was loaded in reference with 800 nM Ca^{2+} (not shown), then immersed in reference with 0 Ca^{2+} (image *A* at 4 s). Release initiation is revealed by the increase in F_3 intensity and the diffusion of Ca^{2+} away from the preparation. Note that there is no abrupt shift in *R* following caffeine introduction to the bathing solution. The reason for this, which is in contrast to that of caffeine in the presence of 5 mM BAPTA (Fig. 6), is not known. However, the shift in *R* was consistent in all fibres exposed to caffeine–BAPTA. No fibres exposed to caffeine–EGTA

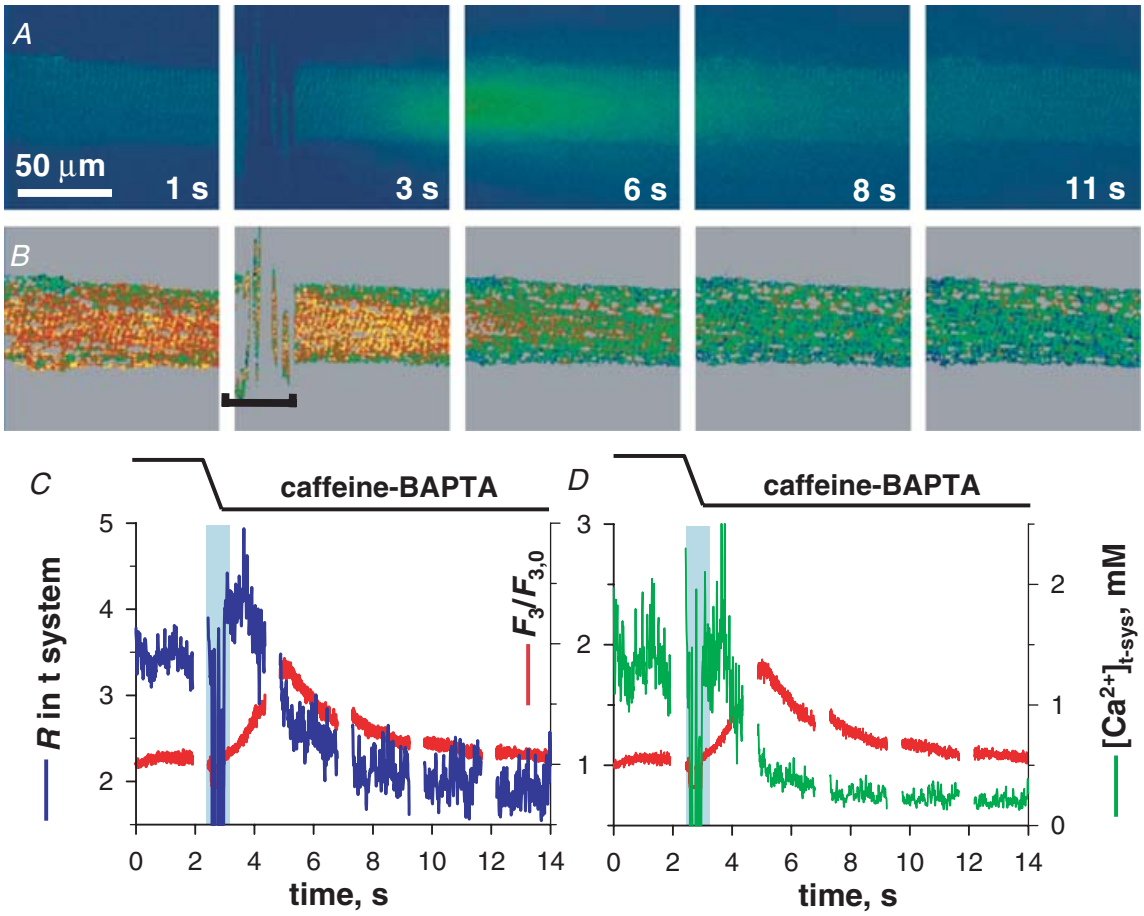

Figure 6. Ca^{2+} movements following Ca^{2+} release in caffeine–BAPTA with moderately Ca^{2+}-loaded SR
A, F_3 and *B*, *R* in t system, acquired while changing from a solution with 5 mM BAPTA, 0 Ca and 0.65 mM Mg^{2+} to releasing-inducing caffeine–BAPTA. *C*, spatially averaged $F_3/F_{3,0}$ (red) and *R* (blue) *versus* elapsed time, which directly correspond to time and *y* axis in *A* and *B*. *D*, spatially averaged $F_3/F_{3,0}$ (red) and $[Ca^{2+}]_{t\text{-}sys}$ (green) derived from *R* in *C*. Note the abrupt shift in *R* at the point of introduction of caffeine in the bathing solution. The calibration of *R* in terms of $[Ca^{2+}]_{t\text{-}sys}$ was done using two sets of measured parameters: one for the period without caffeine (before end of blue bar marking solution change), and the other for the period with caffeine (starting at the end of blue bar). Other details as in Fig. 4. (ID: 072805e_s017.)

displayed the shift. *R* has been calibrated separately under each condition so that $[Ca^{2+}]_{t\text{-}sys}$ can be estimated.

During the rising phase of the caffeine-induced Ca^{2+} transient there was an increase in $[Ca^{2+}]_{t\text{-}sys}$, indicating uptake of Ca^{2+} from the cytoplasm (image *B* at 6 and 8 s). A decrease in $[Ca^{2+}]_{t\text{-}sys}$ followed (image *B* at 13 s), indicating net Ca^{2+} entry presumably due to SOCE. The depletion of $[Ca^{2+}]_{t\text{-}sys}$ continued throughout the recording time, consistent with the lack of recovery of $[Ca^{2+}]_{SR}$ during continued immersion in the same solution (Launikonis *et al.* 2005, 2006).

In order to assess the consequences of t system depolarization on store-dependent Ca^{2+} flux, preparations were loaded in sodium glutamate, high $[Ca^{2+}]$-loading solution and incubated in a Na^{+} reference solution with 0 Ca immediately prior to exposure to caffeine–depol. An example is shown in Fig. 8. A large release of Ca^{2+}, indicated by the increase in cytosolic rhod-2 fluorescence ensued upon exposure to caffeine–depol, and $[Ca^{2+}]_{t\text{-}sys}$ initially increased during the rising phase of the Ca^{2+} transient. $[Ca^{2+}]_{t\text{-}sys}$ began to decrease close to the peak of the Ca^{2+} transient indicating activation of SOCE.

$[Ca^{2+}]_{t\text{-}sys}$ and Ca^{2+} entry flux

The t system fluxes measured above, in conjunction with present and previous estimates of SR calcium content, confirm the presence of SOCE in this preparation and validate the measurement technique. A qualitative validation consisted of showing a change in direction of the net t system flux concomitant with changes in $[Ca^{2+}]_{SR}$. Specifically, $[Ca^{2+}]_{t\text{-}sys}$ largely fell during release of SR Ca^{2+} and could only recover as $[Ca^{2+}]_{SR}$ increased. This correspondence was demonstrated most clearly by contrasting Ca^{2+} release in caffeine (during which there is no recovery of $[Ca^{2+}]_{SR}$ and none was found in $[Ca^{2+}]_{t\text{-}sys}$) with that caused by low Mg^{2+}, where recovery of $[Ca^{2+}]_{SR}$ after brief release (demonstrated by Launikonis *et al.* 2006) was accompanied by reversal of the net Ca^{2+} flux in the t system (shown here in Fig. 4). This behaviour is diagnostic of SOCE (Parekh & Putney, 2005).

Whenever there is substantial Ca^{2+} uptake by the t system, as in initial stages of a Ca^{2+} transient (e.g. image *A* at 6 s in Fig. 7), it is impossible to separate SOCE from uptake. It is still possible, however, to provide a lower bound for SOCE as the net entry flux after it becomes inward. As an example, the change in net t system flux to negative or inward in Fig. 7 (*B*, image at 11 s) indicates that the store-operated inward flux became dominant at this point. The Ca^{2+} entry flux calculated for the first 1 s after this point was not significantly different from the rate estimated in BAPTA release-inducing solutions at a similar $[Ca^{2+}]_{t\text{-}sys}$ (Figs 5 and 6). Later on, $[Ca^{2+}]_{t\text{-}sys}$ decreased more slowly (Fig. 7, images at and after 16 s).

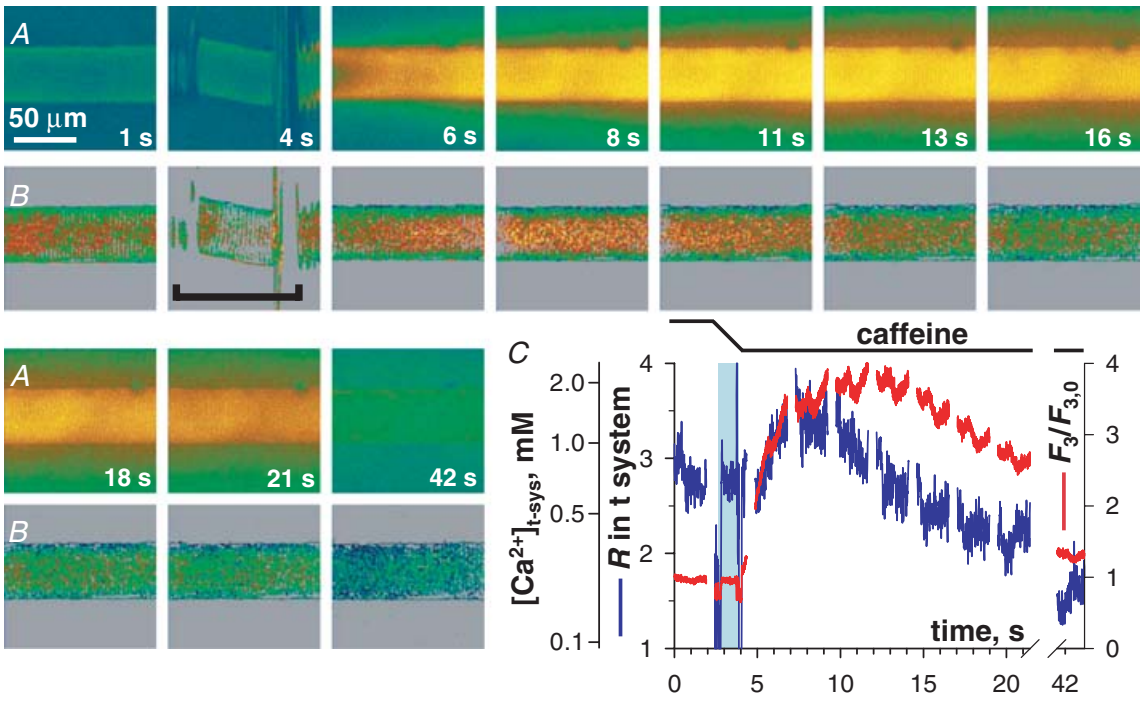

Figure 7. SOCE during complete $[Ca^{2+}]_{SR}$ depletion at resting membrane potential
A, images of rhod-2 fluorescence F_3 and *B*, images of mag-indo-1 *R* in t system, acquired while applying the release-inducing caffeine solution. *C*, spatially averaged $F_3/F_{3,0}$ (red) and *R* (blue) *versus* elapsed time. Other details as in Fig. 4. (ID: 102505e_s010.)

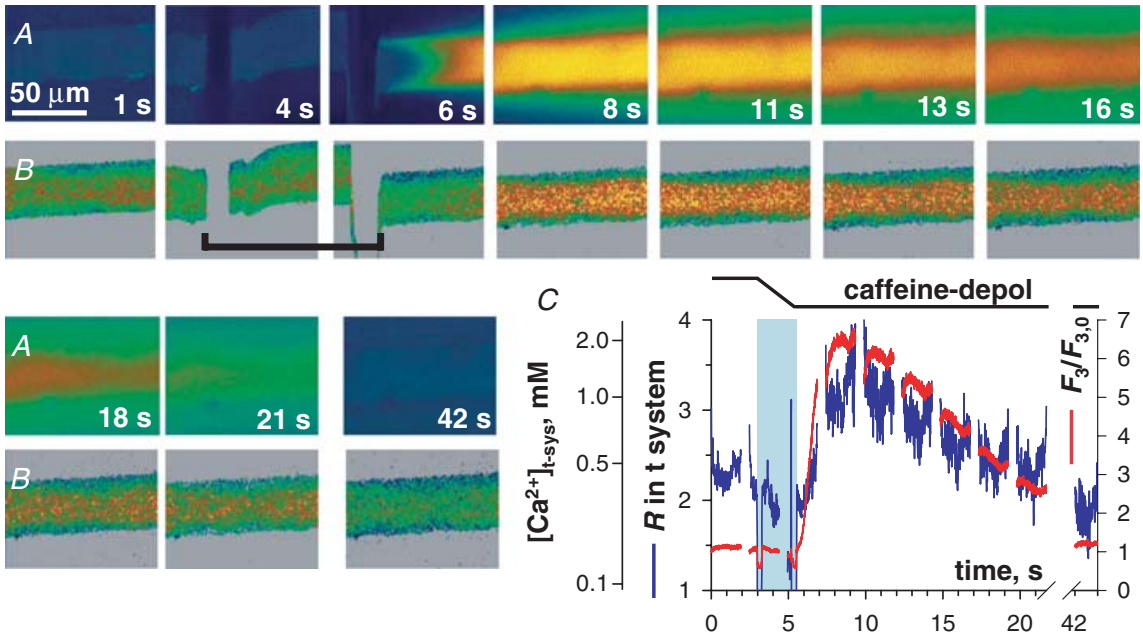

Figure 8. SOCE during complete $[Ca^{2+}]_{SR}$ depletion with a depolarized t system
A, F_3 and *B*, *R* in t system, acquired while applying the release-inducing solution caffeine–depol after transfer from Reference–Na–0 Ca^{2+}, which depolarized the t system. *C*, spatially averaged $F_3/F_{3,0}$ (red) and *R* (blue) *versus* elapsed time. Other details as in Fig. 4. (ID: 092705e_s007.)

The lower rate of decay in the EGTA-buffered solution may be due to (i) Ca^{2+} uptake from the cytoplasm, which would delay the depletion of $[Ca^{2+}]_{t\text{-}sys}$ as the driving force for SOCE declined, or (ii) graded deactivation of SOCE as Ca^{2+} cycled through the SR (Collet & Ma, 2004). It could also be due to a combination of (i) and (ii).

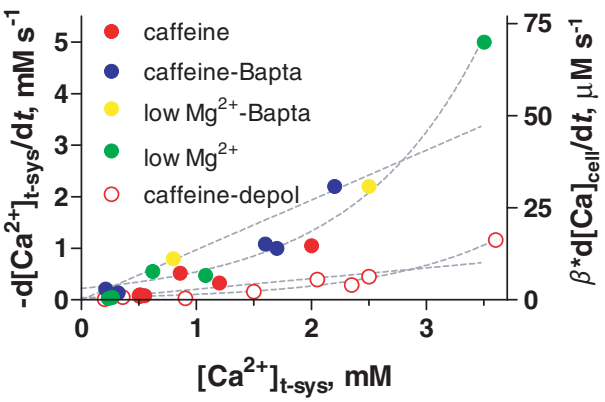

Figure 9. Magnitude of SOCE at different $[Ca^{2+}]_{t\text{-}sys}$ and t system membrane potential
Symbols plot rate of change of $[Ca^{2+}]_{t\text{-}sys}$ *versus* initial value of $[Ca^{2+}]_{t\text{-}sys}$. Right ordinate axis represents rate of change in terms of total cytosolic Ca^{2+} concentration. β is the ratio between total and free t system [calcium]. Colours represent different stimuli as indicated, with filled symbols plotting data obtained with a polarized t system and open symbols a depolarized one. Broken lines plot best linear fits passing through the origin or exponential fits. Best fit parameters: slopes of linear regressions were 0.97 ± 0.02 and 0.21 ± 0.01 s^{-1}; and rate constants for exponentials: 0.90 ± 0.05 and 0.92 ± 0.07 s^{-1}, for polarized and depolarized cells, respectively. $n = 16$ fibres.

The rate of SOCE can now be determined within this framework and used to establish the influence of $[Ca^{2+}]_{t\text{-}sys}$ on store-operated flux. This was done by plotting the rate of decrease of $[Ca^{2+}]_{t\text{-}sys}$ *versus* $[Ca^{2+}]_{t\text{-}sys}$ at the initiation of the event. A summary of results obtained with various release-inducing solutions is in Fig. 9. The curves represent best fits with linear or exponential functions. Intriguingly, the exponentials gave better fits at both membrane potentials. This analysis of collected data clearly demonstrates the following features: the rate of Ca^{2+} flux was significantly greater in normally polarized cells compared to that in depolarized cells. The store-operated Ca^{2+} flux calculated from each release-inducing solution (a minimum estimate, as it assumes equality of net and unidirectional flux) appeared to define a single-valued function of $[Ca^{2+}]_{t\text{-}sys}$, which is both an indication of a simple mechanism (i.e. not dependent on additional, uncontrolled variables) and an indirect validation of the method of calculating this flux. The apparent nonlinearity of the dependence suggests that $[Ca^{2+}]_{t\text{-}sys}$ could have gating (Hofer, 2005), in addition to flux-driving effects, or reflect quantification errors.

The axis on the right side is proportionally calibrated in terms of accessible cytoplasmic volume, assuming a fractional t system volume of 1.4% (Eisenberg, 1983; Dulhunty, 1984; Launikonis & Stephenson, 2002*a*). It is worth noting that the fractional volume of the

t-system ($t\text{-}sys_{vol}$) of intact fibres has been estimated from electron and confocal microscopy, with differing results. The upper estimate for $t\text{-}sys_{vol}$ from electron microscopy in mammalian fast-twitch muscle is 0.7% (Dulhunty, 1984), whereas confocal microscopy estimates 1.4% (Launikonis & Stephenson, 2002*a*). As fibres must be fixed in hypertonic solution for electron microscopy imaging, a correction for shrinkage of the preparation was made from measurements of total fibre volume changes in hypertonic solution, with the assumption that the fibre and t-system volumes shrink proportionally (Eisenberg, 1983). This assumption was found to be incorrect (Launikonis & Stephenson, 2004). Accordingly, fluorescent dyes equilibrated in the t-system of intact, living muscle cells report significantly larger volumes than those estimated from electron microscopy (Endo, 1966; Soeller & Cannell, 1999; Launikonis & Stephenson, 2002*a*).

The flux rates will scale up after taking into account Ca^{2+} buffering within the t system wall (see Methods). This buffering power ($\beta = [\text{total calcium}]_{t\text{-}sys}/[Ca^{2+}]_{t\text{-}sys}$) has not been determined under the present experimental conditions. Under somewhat comparable conditions, with SOCE activated upon depletion of SR Ca^{2+} by 30 mM caffeine, assays of total calcium in the t system put β in the range 1–20 (Donoso *et al.* 1995; Owen *et al.* 1997; M. Barnes and D. G. Stephenson, unpublished observations).

Discussion

SOCE during Ca^{2+} release in skinned fibres

By combining confocal measurements of free $[Ca^{2+}]$ within the t system and simultaneous recordings of cytoplasmic Ca^{2+} we were able to measure for the first time the t system SOCE flux during Ca^{2+} release from the SR in skeletal muscle.

In this study we build on previous work where it was shown that Ca^{2+}-dependent t system fluorescence is an indicator of SOCE in skinned skeletal muscle fibres (Launikonis *et al.* 2003). Depletion of SR Ca^{2+} by application of caffeine caused t system Ca^{2+} to deplete, showing activation of SOCE. By disrupting the coupling between the t system and SR membranes (Lamb *et al.* 1995) the signal to open the SOC channel upon store depletion is severed (Launikonis *et al.* 2003). Because uncoupling interrupts signalling between membranes but does not affect membrane protein function, it is a more precise method of identifying SOCE than the use of a non-specific pharmacological agent, like 2-APB.

It was indeed found that 2-APB interacts with RyR1 in our skinned fibre experiments. This interaction has not been reported in intact fibres. In intact fibre studies the approach is usually to deplete SR Ca^{2+} in the absence of extracellular Ca^{2+} and 2-APB, and then introduce extracellular Ca^{2+} (or the Ca^{2+} surrogate Mn^{2+}) to evoke SOCE and 2-APB to block it. An interaction of 2-APB and RyR1 would go unnoticed in such an experiment. Alternatively, the diffusional access of 2-APB to the triad could be restricted in intact compared to skinned fibres, consequently preventing 2-APB access to RyR1, together with its interfering with Ca^{2+} release.

The current results show $[Ca^{2+}]_{t\text{-}sys}$ changes during Ca^{2+} release. Most notably, low Mg^{2+}-induced Ca^{2+} release resulted in an increase in $[Ca^{2+}]_{t\text{-}sys}$, then an abrupt drop, followed by a recovery as Ca^{2+} release ended (Fig. 4). This sequence occurred in the order of seconds. These changes in $[Ca^{2+}]_{t\text{-}sys}$ can only be due to the net flux of Ca^{2+} across the t system membrane. Therefore, these changes in $[Ca^{2+}]_{t\text{-}sys}$ indicate Ca^{2+} uptake into the t system during Ca^{2+} release from SR, SOCE activation in less than 1 s following initiation of Ca^{2+} release and SOCE termination as the SR refills with Ca^{2+} at the decline of the Ca^{2+} release transient (as demonstrated by Launikonis *et al.* 2006) to allow net reuptake of Ca^{2+} by the t system. This first demonstration of activation and termination of SOCE during a single Ca^{2+} release event in muscle shows that activation of SOCE is rapid under these circumstances.

Ca^{2+} uptake by the t system

A striking observation of this study was that the t system could take up Ca^{2+} during Ca^{2+} release from SR at a rapid rate (up to 1 mM s^{-1} relative to t system volume; Fig. 4). This therefore represents a possible means of Ca^{2+} depletion in the cell during Ca^{2+} release. It would be difficult, however, to extrapolate from these observations to a physiological situation, to for instance estimate Ca^{2+} loss during a train of action potentials that cause fatigue. On the one hand, the present conditions may overestimate the rate of Ca^{2+} loss, as t system Ca^{2+} uptake was observed during a very large release of Ca^{2+} following direct activation of the SR RyR (Figs 4–8). On the other hand, the present measurements amount to a lower limit of Ca^{2+} loss during a comparable Ca^{2+} transient, as intact fibres would allow diffusional efflux from tubules to extracellular space, which would reduce the t system concentration buildup and enhance Ca^{2+} efflux into the t system.

Properties of SOCE in muscle

This study demonstrates three features of SOCE: (i) it does not require complete depletion of the SR, (ii) its activation and rate are approximately independent of the magnitude of the cytoplasmic Ca^{2+} transient, and (iii) it is activated by local SR depletion. (i) follows from the fact that SOCE was activated prior to the peak of the Ca^{2+} transients (Figs 4–8), indicating that Ca^{2+} was still present in the SR at the time of activation. This observation, plus the similarity of fluxes with different degrees of

cytosolic buffering, constitutes evidence that $[Ca^{2+}]_c$ is not a direct determinant or mediator of SOCE in muscle. The local character of activation of SOCE was shown by the spatially inhomogeneous decrease in $[Ca^{2+}]_{t\text{-}sys}$ associated with a non-uniform release of Ca^{2+} from SR across the fibre (Figs 4–6).

Importantly, activation of SOCE was observed to occur locally in less than 1 s following the introduction of release-inducing solutions containing 5 mM BAPTA. Furthermore, activation of SOCE occurred throughout the whole t system, consistent with the spatiotemporal pattern of SR Ca^{2+} depletion, which was dependent on the rate of Mg^{2+} diffusion away from the preparation (Figs 4–6). By comparison with recent studies of SOCE activation in the small, non-excitable Jurkat cell (Wu *et al.* 2006; Luik *et al.* 2006), we can further elucidate the mechanism of SOCE activation in skeletal muscle. Following Ca^{2+} depletion of ER in Jurkat cells there is accumulation of the intra-store Ca^{2+} sensor STIM1 (stromal interacting molecule 1) at junctional regions of the ER. The subsequent SOC channel activation takes place only at specific sites on the surface membrane (Luik *et al.* 2006). This process required one-third of junctional ER to relocate to the plasma membrane in an overall process taking 6–10 s to reach 20% maximal activation (Wu *et al.* 2006). Therefore the time required to reach maximal SOCE activation in mammalian skeletal muscle (Fig. 5) was more than an order of magnitude shorter than that required to reach 20% maximal activation in Jurkat cells.

The contrasting properties of skeletal muscle, where junctional SR is structurally static and activation of SOCE is faster and spatially unrestricted in the t system, suggest that the elementary molecular machinery for SOCE in skeletal muscle is already uniformly distributed and present in the junctional membranes prior to store depletion. A direct physical interaction between the relevant molecules is plausible given that this cell already has the well-defined contacts between the t system and SR that drive EC coupling (Franzini-Armstrong *et al.* 1999; Paolini *et al.* 2004). This model is also consistent with the functional disruption of SOCE caused in skeletal muscle by high intracellular $[Ca^{2+}]$ treatment, which severs the protein–protein interactions between the SR and t system at the triad (Launikonis *et al.* 2003).

In contrast to studies of non-excitable cells (Hoth & Penner, 1993; Zweifach & Lewis, 1995), we found termination of SOCE to be independent of cytoplasmic Ca^{2+} conditions but fully regulated from the SR. This is consistent with the observation (Kurebayashi & Ogawa, 2001) of a prolonged rise of $[Ca^{2+}]_c$ due to SOCE, reaching micromolar levels without inactivation, in an intact skeletal muscle cell in the presence of a SR Ca^{2+}-pump inhibitor. The difference with the inactivation properties described in non-excitable cells may reflect different store-operated currents (I_{CRAC} and I_{SOC}; Parekh & Putney, 2005; Lewis, 2007). In skeletal muscle, an I_{CRAC} with Ca^{2+} inactivation properties similar to those described in non-excitable cells is yet to be reported. The differences seem teleologically justified. In working muscle, where $[Ca^{2+}]_c$ can reach tens of micromolar (Baylor & Hollingworth, 2003), entry flux should be able to proceed independently of the increase in $[Ca^{2+}]_c$ in order to maintain a required level of $[Ca^{2+}]_{SR}$.

Ca^{2+} entry flux rate

This study provides the first determination of Ca^{2+} entry flux rates during Ca^{2+} release in skeletal muscle cells. Ca^{2+} entry flux during Ca^{2+} release was found to be dependent on the driving force provided by $[Ca^{2+}]_{t\text{-}sys}$ and the membrane potential (Fig. 9), even though the dependence was not linear as simple permeation theory would predict. In any case, the physiological conditions in skeletal muscle of 2 mM $[Ca^{2+}]_{t\text{-}sys}$ and a membrane potential of around −90 mV will strongly favour inward Ca^{2+} flux to the cell when SOC channels are activated in skeletal muscle.

From the results summarized in Fig. 9, the SOCE flux in the resting cell at 2 mM $[Ca^{2+}]_{t\text{-}sys}$ (relative to t-system volume) can be estimated at 18.6 μM s^{-1} (in terms of the accessible cytoplasmic volume) times the buffering power of the t system, a factor in the range 1–20 (see Methods; Hidalgo *et al.* 1986; Owen *et al.* 1997). This can be compared with estimates from studies on intact cells, according to which it takes 1–2 min to refill the depleted SR following reintroduction of 2 mM extracellular Ca^{2+} (Kurebayashi & Ogawa, 2001; Collet & Ma, 2004). The rate of SOCE measured here at physiological $[Ca^{2+}]_{t\text{-}sys}$ predicts that 1.12–2.24 mM calcium will enter the cell in 1–2 min, which should be sufficient to refill the SR of mammalian fibres (1.01 mM total calcium concentration; Fryer & Stephenson, 1996) even if graded deactivation of SOCE slowed the influx rate as the SR refilled (Collet & Ma, 2004).

These observations and calculations confirm the presence of SOCE and show that its flux across the t system can fully account for the SR refilling times in intact cells (Kurebayashi & Ogawa, 2001). Recently, though, the existence of SOCE in skeletal muscle fibres has been brought into question by Allard *et al.* (2006). This group used a combination of voltage- and patch-clamping techniques to monitor electrical activity across the surface membrane during Ca^{2+} release from SR. In this work the major part of the cell was electrically insulated with silicone grease allowing accurate control of voltage in the exposed area (a 100 μm segment of a ∼30 μm diameter cell). In contrast to the results of others (Vandebrouck *et al.* 2002), no unitary channel activity was recorded across a patch of the exposed sarcolemma during depleting Ca^{2+} release. The result was interpreted as evidence

for either the absence of SOCE across this membrane, or for it consisting of unitary currents of undetectable size.

Moreover, the macroscopic current recorded by Allard *et al.* (2006) under voltage-clamp upon repolarization from long Ca^{2+}-depleting pulses did not change in a significant way, suggesting that there was no SOCE across the t system either, and similarly minor changes in current were observed after other treatments that caused cell-wide depletion. These apparently negative results are not inconsistent with the presence of an electrogenic SOCE with the magnitude reported here. Indeed, the Ca^{2+} current density associated with a flux of 1 mM per minute, about 3.2 A l^{-1}, would result in a macroscopic current of ~0.3 nA in the cell segments used by Allard *et al.* (2006). Changes of that magnitude could have passed unnoticed, given the evident presence of other electrophysiological changes upon various treatments (e.g. their Fig. 1). In fact, after 5 min of application of cyclopiazonic acid, which caused a substantial loss of SR calcium, the incremental current in response to a −100 mV pulse increased by ~0.2 A F^{-1}, or 0.2 nA in a 1000 pF cell (Fig. 5 of Allard *et al.* 2006). In this framework it is possible to conclude that SOCE is controlled at the triads and not across the sarcolemma in skeletal muscle. However, the experiments of Allard *et al.* do not fully disprove the presence of SOCE across the sarcolemma, leaving this controversy unresolved.

Other studies of SOCE in skinned fibres (Zhao *et al.* 2005, 2006; Hirata *et al.* 2006) suggest a much slower entry flux than observed here, with the t system taking up to 12 min to deplete of Ca^{2+} upon store depletion. In sharp contrast, all entry fluxes reported in our study ended in seconds, by deactivation of SOCE or t system depletion.

Several technical differences may account for the discrepancies: in the studies referred to above, all cells were probed for their SOCE response in a K^+-based internal solution with no Na^+, thus rendering the t system Na^+ pump inactive and depolarizing the t system. This feature alone does not account for the difference, however, because the depolarized cells of our study still depleted calcium in the t system in less than 1 min following store depletion (Fig. 8). In the previous studies attempts to deplete SR Ca^{2+} were done with caffeine in the presence of ~1 mM $[Mg^{2+}]_c$ and submillimolar [ATP], without an indicator of SR Ca^{2+} release. Caffeine is a poor activator of RyR1 in adult skeletal muscle at 1 mM $[Mg^{2+}]_c$ (Lamb *et al.* 2001) and at low [ATP] (Owen *et al.* 1996; Laver *et al.* 2001; Dutka & Lamb, 2004). Therefore store depletion, which was not demonstrated under the conditions used, may have been limited, and most significantly, in the previous studies fibres were skinned in a solution with 0.5 mM total calcium and 0.5 mM rhod-5N (Zhao *et al.* 2005; Hirata *et al.* 2006), which exposed skinned fibres to micromolar levels of Ca^{2+}. In addition, skinned fibres were further exposed to micromolar levels of Ca^{2+} for several minutes in order to load the t system and SR (Zhao *et al.* 2005). The exposure of the intracellular environment to micromolar Ca^{2+} for a few minutes irreversibly disrupts the coupling between the t system and SR membranes (Lamb *et al.* 1995; Launikonis *et al.* 2003; Verburg *et al.* 2005).

Preliminary results from another laboratory employing skinned fibres to study SOCE in mammalian muscle have also appeared (Duke & Steele, 2006). They report that fluorescence of t system-trapped fluo-5N of rat fibres is lost in less than 1 min following waves of Ca^{2+} release induced in an internal solution with halothane and low Mg^{2+}. This rate of SOCE is consistent with that presented here and with the levels previously shown in amphibian skeletal muscle (Launikonis *et al.* 2003).

$[Ca^{2+}]_{SR}$ and activation of SOCE in skeletal muscle

Problems finding a protocol suitable to load Ca^{2+} into the t system while achieving an endogeneous level of Ca^{2+} in SR (Fryer & Stephenson, 1996) meant that Ca^{2+} probably exceeded normal levels in some fibres. Given the fact that SOCE was clearly active prior to complete depletion of Ca^{2+} in SR (Figs 4–8), the question remains open whether SOCE has a relative or absolute threshold in skeletal muscle. That is, can SOCE start following release of a certain amount of Ca^{2+} from SR regardless of the initial level or does a certain level of Ca^{2+} depletion in SR have to be reached for activation?

In summary, we have shown that store-dependent Ca^{2+} influx across the t system can be measured during Ca^{2+} release in rat skeletal muscle. SOCE flux determined this way was much higher than in earlier estimates, at values consistent with the rapid refilling of the cellular stores demonstrated in intact cells. SOCE flux was also found to be strongly dependent on the membrane potential and Ca^{2+} gradient. From our observations of SOCE in these experiments we present a model of SOCE in skeletal muscle where the elementary molecular units of SOCE are evenly distributed throughout the t system and are locally controlled, activated rapidly following Ca^{2+} release and influenced little by changes in cytosolic $[Ca^{2+}]$ within the physiological range but fully regulated from within the SR.

References

Allard B, Couchoux H, Pouvreau S & Jacquemond V (2006). Sarcoplasmic reticulum Ca^{2+} release and depletion fail to affect sarcolemmal ion channel activity in mouse skeletal muscle. *J Physiol* **575**, 68–81.

Almers W, Fink RHA & Palade PT (1981). Calcium depletion in frog muscle tubules: the decline of calcium current under maintained depolarization. *J Physiol* **312**, 177–207.

Baylor SM & Hollingworth S (2003). Sarcoplasmic reticulum calcium release compared in slow-twitch and fast-twitch fibres of mouse muscle. *J Physiol* **551**, 125–138.

Cheung A, Dantzig JA, Hollingworth S, Baylor SM, Goldman YE, Mitchison TJ & Straight AF (2002). A small-molecule inhibitor of skeletal muscle myosin II. *Nat Cell Biol* **4**, 83–88.

Collet C & Ma J (2004). Calcium-dependent facilitation and graded deactivation of store-operated calcium entry in fetal skeletal muscle. *Biophys J* **87**, 268–275.

Di Biase V & Franzini-Armstrong C (2005). Evolution of skeletal type e-c coupling: a novel means of controlling calcium delivery. *J Cell Biol* **171**, 695–704.

Donoso P, Prieto H & Hidalgo C (1995). Luminal calcium regulates calcium release in triads isolated from frog and rabbit skeletal muscle. *Biophys J* **68**, 507–515.

Duke AM & Steele D (2006). Store-operated Ca^{2+} entry following halothane-induced Ca^{2+} waves in mechanically skinned rat muscle fibres. *Proc Physiol Soc* **3**, 140P.

Dulhunty AF (1984). Heterogeneity of t-tubule geometry in vertebrate skeletal muscle fibres. *J Muscle Res Cell Mot* **5**, 333–347.

Dutka TL & Lamb GD (2004). Effect of low cytoplasmic [ATP] on excitation-contraction coupling in fast-twitch muscle fibres of the rat. *J Physiol* **560**, 451–468.

Eisenberg BR (1983). Quantitative ultrastructure of mammalian skeletal muscle. In *Handbook of Physiology*, section 10, *Skeletal Muscle*, ed. Peachey LD, pp. 73–112. American Physiological Society, Bethesda, MD, USA.

Endo M (1966). Entry of fluorescent dyes into the sarcotubular system of the frog muscle. *J Physiol* **185**, 224–238.

Franzini-Armstrong CA, Protasi F & Ramesh V (1999). Shape, size, and distribution of Ca^{2+} release units and couplons in skeletal and cardiac muscle. *Biophys J* **77**, 1528–1539.

Friedrich O, Ehmer T, Uttenweiler D, Vogel M, Barry PH & Fink RHA (2001). Numerical analysis of Ca^{2+} depletion in the transverse tubular system of mammalian muscle. *Biophys J* **80**, 2046–2055.

Fryer MW & Stephenson DG (1996). Total and sarcoplasmic reticulum calcium contents of skinned fibres from rat skeletal muscle. *J Physiol* **493**, 357–380.

Grynkiewicz G, Poenie M & Tsien RY (1985). A new generation of Ca^{2+} indicators with greatly improved fluorescence properties. *J Biol Chem* **260**, 3440–3450.

Herrmann-Frank A, Luttgau H-C & Stephenson DG (1999). Caffeine and excitation-contraction coupling in skeletal muscle: a stimulating story. *J Muscle Res Cell Motil* **20**, 223–237.

Hidalgo C, Cifuentes F & Donoso P (1991). Sodium-calcium exchange in transverse tubule vesicles isolated from amphibian skeletal muscle. *Ann NY Acad Sci* **639**, 483–497.

Hidalgo C, González ME & García AM (1986). Calcium transport in transverse tubules isolated from rabbit skeletal muscle. *Biochim Biophys Acta* **854**, 279–286.

Hirata Y, Brotto M, Weisleder N, Chu Y, Lin P, Zhao X, Thornton A, Komazaki S, Takeshima H, Ma J & Pan Z (2006). Uncoupling store-operated Ca^{2+} entry and altered Ca^{2+} release from sarcoplasmic reticulum through silencing of junctophilin genes. *Biophys J* **90**, 4418–4427.

Hofer AM (2005). Another dimension to calcium signaling: a look at extracellular calcium. *J Cell Sci* **118**, 855–862.

Hoth M & Penner R (1993). Calcium release-activated calcium current in rat mast cells. *J Physiol* **465**, 737–749.

Kurebayashi N & Ogawa Y (2001). Depletion of Ca^{2+} in the sarcoplasmic reticulum stimulates Ca^{2+} entry into mouse skeletal muscle fibres. *J Physiol* **533**, 185–199.

Lamb GD, Cellini MA & Stephenson DG (2001). Different Ca^{2+} releasing action of caffeine and depolarization in skeletal muscle fibres of the rat. *J Physiol* **531**, 715–728.

Lamb GD, Junankar PR & Stephenson DG (1995). Raised intracellular [Ca^{2+}] abolishes excitation–contraction coupling in skeletal muscle fibres of rat and toad. *J Physiol* **489**, 349–362.

Lamb GD & Stephenson DG (1990). Calcium release in skinned muscle fibres of the toad by transverse tubule depolarization or by direct stimulation. *J Physiol* **423**, 495–517.

Lamb GD & Stephenson DG (1994). Effects of intracellular pH and [Mg^{2+}] on excitation–contraction coupling in skeletal muscle fibres of the rat. *J Physiol* **478**, 331–339.

Launikonis BS, Barnes M & Stephenson DG (2003). Identification of the coupling between skeletal muscle store-operated calcium entry and the inositol trisphosphate receptor. *Proc Natl Acad Sci U S A* **100**, 2941–2944.

Launikonis BS & Stephenson DG (2000). Effects of Mg^{2+} on Ca2+ release from sarcoplasmic reticulum of skeletal muscle fibres from yabby (crustacean) and rat. *J Physiol* **526**, 299–312.

Launikonis BS & Stephenson DG (2002*a*). Tubular system volume changes in twitch fibres from toad and rat skeletal muscle assessed by confocal microscopy. *J Physiol* **538**, 607–618.

Launikonis BS & Stephenson DG (2002*b*). Properties of the vertebrate skeletal muscle tubular system as a sealed compartment. *Cell Biol Int* **26**, 921–929.

Launikonis BS & Stephenson DG (2004). Osmotic properties of the sealed tubular system of toad and rat skeletal muscle. *J Gen Physiol* **123**, 231–247.

Launikonis BS, Zhou J, Royer L, Shannon TR, Brum G & Ríos E (2005). Confocal imaging of [Ca^{2+}] in cellular organelles by SEER, shifted excitation and emission ratioing. *J Physiol* **567**, 523–543.

Launikonis BS, Zhou J, Royer L, Shannon TR, Brum G & Ríos E (2006). Depletion 'skraps' and dynamic buffering inside the cellular Ca^{2+} store. *Proc Natl Acad Sci U S A* **103**, 2982–2987.

Laver DR, Lenz GKE & Lamb GD (2001). Regulation of the calcium release channel from rabbit skeletal muscle by the nucleotides ATP, AMP, IMP and adenosine. *J Physiol* **537**, 763–778.

Lewis RS (2007). The molecular choreography of a store-operated calcium channel. *Nature* **446**, 284–287.

Luik RM, Wu MW, Buchanan J & Lewis RS (2006). The elementary unit of store-operated Ca^{2+} entry: local activation of CRAC channels by STIM1 at ER-plasma membrane junctions. *J Cell Biol* **174**, 815–825.

McKemy DD, Welch W, Airey JA & Sutko JL (2000). Concentrations of caffeine greater than 20 mM increase the indo-1 fluorescence ratio in a Ca^{2+}-independent manner. *Cell Calcium* **27**, 117–124.

Melzer W, Herrmann-Frank A & Luttgau HC (1995). The role of Ca^{2+} ions in excitation-contraction coupling of skeletal muscle fibres. *Biochim Biophys Acta* **1241**, 59–116.

Muschol M, Dasgupta BR & Salzberg BM (1999). Caffeine interaction with fluorescent calcium indicator dyes. *Biophys J* **77**, 577–586.

Owen VJ, Lamb GD & Stephenson DG (1996). Effect of low [ATP] on depolarization-induced Ca^{2+} release in skeletal muscle of the toad. *J Physiol* **493**, 309–315.

Owen VJ, Lamb GD, Stephenson DG & Fryer MW (1997). Relationship between depolarization-induced force responses and Ca^{2+} content in skeletal muscle fibres of rat and toad. *J Physiol* **498**, 571–586.

Paolini C, Fessenden JD, Pessah IN & Franzini-Armstrong C (2004). Evidence for conformational coupling between two calcium channels. *Proc Natl Acad Sci U S A* **101**, 12748–12752.

Parekh AB & Putney JW Jr (2005). Store-operated calcium channels. *Physiol Rev* **85**, 757–810.

Posterino GS & Lamb GD (2003). Effect of sarcoplasmic reticulum Ca^{2+} content on action potential-induced Ca^{2+} release in rat skeletal muscle fibres. *J Physiol* **524**, 239–258.

Pouvreau S, Royer L, Yi J, Brum G, Meissner G, Ríos E & Zhou J (2007). Ca^{2+} sparks operated by membrane depolarization require isoform 3 ryanodine receptor channels in skeletal muscle. *Proc Natl Acad Sci U S A* **104**, 5235–5240.

Rome LC (2006). Design and function of superfast muscles: new insights into physiology of skeletal muscle. *Annu Rev Physiol* **68**, 193–221.

Sacchetto R, Margreth A, Pelosi M & Carafoli E (1996). Colocalization of the dihydropyridine receptor, the plasma-membrane calcium ATPase isoform 1 and the sodium/calcium exchanger to the junctional-membrane domain of transverse tubules of rabbit skeletal muscle. *Eur J Biochem* **237**, 483–488.

Shirokova N, García J, Pizarro G & Ríos E (1996). Ca^{2+} release from the sarcoplasmic reticulum compared in amphibian and mammalian skeletal muscle. *J Gen Physiol* **107**, 1–18.

Shirokova N, García J & Ríos E (1998). Local calcium release in mammalian skeletal muscle. *J Physiol* **512**, 377–384.

Soeller C & Cannell MB (1999). Examination of the transverse tubular system in living cardiac rat myocytes by 2-photon microscopy and digital image-processing techniques. *Circ Res* **84**, 266–275.

Stephenson DG & Lamb GD (1993). Visualisation of the transverse tubular system in isolated intact and in mechanically skinned muscle fibres of the cane toad by confocal laser scanning microscopy. *J Physiol* **459**, 15*P*.

Stern MD, Pizarro G & Ríos E (1997). Local control model of excitation-contraction coupling in skeletal muscle. *J Gen Physiol* **110**, 415–440.

Vandebrouck C, Martin D, Colson-Van Schoor M, Debaix H & Gailly P (2002). Involvement of TRPC in the abnormal calcium influx observed in dystrophic (mdx) mouse skeletal muscle. *J Cell Biol* **158**, 1089–1096.

Veratti E (1961). Investigations on the fine structure of striated muscle fiber. *J Biophys Biochem Cytol* **10**, 1–59.

Verburg E, Murphy RM, Stephenson DG & Lamb GD (2005). Disruption of excitation–contraction coupling and titin by endogenous Ca^{2+}-activated proteases in toad muscle fibres. *J Physiol* **564**, 775–790.

Wu MW, Buchanan J, Luik RM & Lewis RS (2006). Ca^{2+} store depletion causes STIM1 to accumulate in ER regions closely associated with the plasma membrane. *J Cell Biol* **174**, 803–813.

Zhao X, Weisleder N, Han X, Pan Z, Parness J, Brotto M & Ma J (2006). Azumolene inhibits a component of store-operated calcium entry coupled to the skeletal muscle ryanodine receptor. *J Biol Chem* **281**, 33477–33486.

Zhao X, Yoshita M, Brotto L, Takeshima H, Weisleder N, Hirata Y, Nosek TM, Ma J & Brotto M (2005). Enhanced resistance to fatigue and altered calcium handling properties of sarcalumenin knockout mice. *Physiol Genomics* **23**, 72–78.

Zhou J, Launikonis BS, Ríos E & Brum G (2004). Regulation of Ca^{2+} sparks by Ca^{2+} and Mg^{2+} in mammalian and amphibian muscle. An RyR isoform-specific role in excitation–contraction coupling? *J Gen Physiol* **124**, 409–428.

Zweifach A & Lewis RS (1995). Rapid inactivation of depletion-activated calcium current (I_{CRAC}) due to local calcium feedback. *J Gen Physiol* **105**, 209–226.

Acknowledgements

We thank D.G. Stephenson (La Trobe University) for comments on the manuscript. B.S.L. was a C. J. Martin Fellow of the National Health and Medical Research Council (Australia). This work was supported by grants from National Institute of Arthritis and Musculoskeletal and Skin Diseases/National Institute of Health to E. Ríos.

Supplemental material

Online supplemental material for this paper can be accessed at:
http://jp.physoc.org/cgi/content/full/jphysiol.2007.135046/DC1
and
http://www.blackwell-synergy.com/doi/suppl/10.1113/jphysiol.2007.135046